www.amlett.com, www.vbripress.com/aml, DOI: 10.5185/amlett.2015.5606 Published online by the VBRI press in 2015

Growth and properties of pulsed laser deposited Al-doped ZnO thin film

Gurpreet Kaur*, Anirban Mitra, K.L. Yadav

High Power Laser Lab, Department of Physics, Indian Institute of Technology Roorkee, Roorkee-247667, Uttarakhand, India

*Corresponding author. E-mail: physk@gmail.com

Received: 30 July 2014, Revised: 12 September 2014 and Accepted: 24 October 2014

ABSTRACT

Al-doping of 1.5% by weight, in ZnO (Al:ZnO), thin films are deposited on glass substrates at temperature 400 °C and varying oxygen gas pressure (PO_2) from 1.33 Pa to 5.32 Pa via Pulsed Laser Deposition (PLD) technique. The single crystalline nature of the thin films is confirmed from the X-ray diffraction (XRD) pattern. The evaluated crystallite size is found to be <15 nm. Atomic Force Microscopy (AFM) study reveals the columnar grain formation in the thin films, with low surface roughness. The surface morphology of the grown thin films is significantly affected by PO_2. Optical measurements depict that the thin films are highly transparent in the visible region with transmittance up to 80%. The optical band gap calculated from Tauc's plot evinced that Al-doping results in band edge bending in Al:ZnO thin films, a red shift in the band gap is observed with increase in PO_2 that is due to the contributing electrons from oxygen ions. Photoluminescence (PL) spectra of films indicate the visible emission peaks originating from defect states. Optical properties of the thin films confirm their applicability for optoelectronic devices. The room temperature, current-voltage (I-V) plots indicate low resistivity in the thin films ~ 10^{-2} (Ω-cm). Copyright © 2015 VBRI Press.

Keywords: Pulsed laser deposition; Al-doped ZnO (Al:ZnO) thin film; transmittance; Tauc's plot; band gap.

Gurpreet Kaur did her postgraduate in Physics from 'Guru Nanak Dev University, Amritsar, India' in the year of 2010. Currently she is doing Ph.D. in Physics (Experimental condensed matter) in Indian Institute of Technology Roorkee, India. She is working on Pulsed laser deposition (PLD) technique to fabricate oxide thin films and their applicability for optical devices.

Anirban Mitra received his Ph.D degree from Indian Institute of Technology, Kanpur, India in Physics in the year 2002. He then moved to Institute of Laser Engineering, Osaka University, Japan as Research Associate and worked there till 2004. In 2004 he had joined Department of Physics, Trinity College, Dublin, Ireland as Post Doctoral Researcher and then moved to Dublin City University in the year 2005. In 2006 he came back to India and in 2007 joined Kalinga Institute of Industrial Technology, Bhubaneswar as Assistant Professor. He had joined Department of Physics, Indian Institute of Technology, Roorkee in 2008 and since then he is working there as Assistant Professor. His current research area of interest is wide band gap semiconductor and plasmonics.

K.L. Yadav is currently Professor in the Department of Physics, Indian Institute of Technology Roorkee, India. He holds M.Sc. and Ph.D. degree in Physics from Indian Institute of Technology Kharagpur, India in 1989 and 1994, respectively. In 2001, he received BOYSCAST Fellowship at Materials Research Institute, Pennstate University, USA. In addition, he obtained JSPS fellowship at National Institute for Materials Science, Tsukuba, Japan in 2010. In his academic carrier, he has published more than 140 papers in SCI Journals and is an author of one contributory chapter in a book of International level in the field of materials science and technology. His major research interests are Functional Nanomaterials, Multiferroic, Smart Sensors and Biomaterials. His recent research interest is focused on designing and development of smart materials for device applications. He strongly advocates the use of research methodology in the education. His work has been widely read and cited in both academia and industry and one of the papers has been cited 132 times. He is an active member and leader in the Materials Engineering community. He contributes regularly to a number of professional societies (e.g., MRSI, and Discussion Group), journals and universities.

Introduction

Nanostructured thin films have emerged as one of the most promising source to fabricate various devices with significantly enhanced performance characteristics. The quantum phenomena occurring in these materials cause a ballistic jump in their performance and the resulting device finds industrial applications **[1]**. Transparent conducting

 Copyright © 2015 VBRI Press

oxides (TCO) are widely used in optoelectronic devices, thin film solar cells and transparent electrodes in display **[2]**. ZnO is n-type semiconductor with a direct band gap of 3.37 eV and a high exciton binding energy of ~ 60 meV **[3]**. The large band gap energy of ZnO materials would allow for stable high-yield excitonic luminescence from even at room temperature **[4]**. ZnO is considered as most promising material as it is thermally and chemically stable, non toxic and has a low cost **[5]**. To improve the electrical conductivity and transparency of ZnO it is doped with trivalent metal cations such as Al, In, Ga **[5]**. Among the various dopants, Al is considered as an efficient n-type dopant for realizing high quality samples with enhanced band gap, higher conductivity, ultraviolet/blue light emission and good optical transmittance **[6]**. The utmost factors like the electronic-structure, dopant concentration, energy-levels of dopant and d-electronic configuration of the ions that could affect the properties of the resulting compound **[7]**. Al-doped ZnO show good optoelectronic properties, and finds applications in devices such as solar cells and organic light emitting diodes **[8, 2]**. Al:ZnO is also an attractive candidate for ultraviolet (UV) photoconductive sensor applications **[6]**. The optical properties of the grown films depend upon their crystalline nature **[8]**. To employ Al:ZnO thin films for optoelectronic applications with good performance, we have to deposit thin films with good crystalline nature. The crystallinity of the thin films depends upon the optimized deposition parameters such as temperature and pressure and the technique employed. There are various chemical and physical deposition techniques to grow oxide thin films; Pulsed Laser Deposition (PLD) stands out as it retains the stoichiometric nature of multi-component system **[2]**.

In this paper we have focused on the effect of oxygen gas pressure (PO_2) on the growth, structural, optical and electrical properties of Pulsed Laser Deposited, single crystalline Al:ZnO films. The promising photoluminescence (PL) properties are discussed in detail and emphasized on the practical applications of the deposited Al:ZnO thin films.

Experimental

Deposition of the thin films

Al:ZnO thin films are deposited on Soda lime glass substrates in the presence of oxygen gas, using Pulsed Laser Deposition technique (Excel Instruments). The stainless steel vacuum chamber is first evacuated to 10^{-5} Pa the base pressure using a turbo molecular pump backed up with a rotary vacuum pump. We have chosen 1.5% Al-doping by weight in ZnO. The target of Al:ZnO is prepared by the solid state reaction method, via mixing Al_2O_3 (99.998%, Sigma Aldrich) and ZnO (99.998%, Sigma Aldrich) powders in stoichiometric ratios. These homogeneous powders are pressed to form a pallet of diameter 20 mm and thickness of about 5 mm, by applying 20 tons force with a hydraulic press. This pallet is sintered at 1200 °C for 2 hours in a furnace to form the PLD target of Al:ZnO. The chemical reaction of Al_2O_3 and ZnO allows formation of spinel phase $ZnAl_2O_4$ (Al:ZnO). The target is ablated using an Nd-YAG laser operating at wavelength 355 nm, the third harmonic of the laser. The glass substrates are ultrasonically cleaned with acetone and then mounted on the substrate holder provided with a heating stage. The laser operated in the UV energy region is used to ablate the target atoms, and a plasma-plume is formed by the ejected materials containing highly excited and energetic species. The plasma-plume expands isothermally away from the target surface and interacts with the chamber atmosphere and results in the deposition of thin film on the substrate. The most advantageous feature of depositing thin film by PLD is that the laser is used as an external energy source the deposition can occur in both inert and reactive background gases. The deposition rate and the thickness of the deposited thin film are controlled by the laser repetition frequency and the deposition time. We have deposited four thin film samples of thickness 300 nm and keeping the substrate temperature at 400 °C and oxygen gas pressure (PO_2) is varied from 1.33 to 5.32 Pa in steps of 1.33 Pa. The optimized parameters for the growth of Al:ZnO thin films are listed in **Table 1**. To improve the crystallinity of thin films we have done in-situ post deposition annealing for 20 minutes in a vacuum.

Table 1. Optimized deposition parameters for the growth of Al:ZnO thin films.

Optimized deposition parameters for Al:ZnO thin films	
Laser Used	Nd-YAG Laser
Laser Wavelength	355 nm
Laser Energy	150 mJ/pulse
Pulse Repetition Rate	10 Hz
No. of Laser Shots	6,000
Target Used	Al:ZnO target
Gas Used	Oxygen (99.9% purity)
Gas Pressure	1.33 to 5.32 Pa, in steps of 1.33 Pa
Substrate	Glass
Substrate Temperature	400 °C
Target to Substrate Distance	35 mm

Thin films characterizations

The crystal structural characterizations of the deposited thin films are examined by X-ray diffractometer model Bruker AXS D8 Advanced in θ-2θ mode, with CuKα radiation (λ = 0.154 nm). The surface morphology and the roughness of the deposited thin films is examined by Atomic Force Microscopy (NT-MDT: Model NTEGRA), in semi-contact mode provided with a Silicon Nitride tip of radius 10 nm. Optical characterizations of these thin films are done by JASCO Model V-650 spectrophotometer. The band gap of thin films is calculated from Tauc's plot. The Photoluminescence (PL) of the thin films is observed by Spectrofluorophotometer model SHIMADZU-RF-5301PC. The current-voltage (I–V) characteristics from 0-4 V are observed at room temperature using Keithley 2636A dual channel Source major unit sealed in the Black Box and provided with a proper arrangement.

Results and discussion

Structural and morphological properties

Fig. 1 reveals the room temperature XRD patterns of Al:ZnO films grown on glass substrates. The as-deposited Al:ZnO has a diffraction peak at Bragg angle, 2θ = 34.37°.

Copyright © 2015 VBRI Press

The XRD peak is indexed as (002) by comparing the data with JCPDS card file no. 77-0191. The XRD pattern shows a single peak of high intensity for all thin films which implies highly oriented and single crystalline nature of the thin films. The thin films are grown along c-axis with hexagonal wurtzite crystal structure and space group Fm3m(225). The intensity of the XRD peak describes the crystalline quality of the thin films, better is the crystallinity for more intense peak. The interplanar distance, d is calculated using Bragg's law equation: 2d sin(θ) = nλ. For hexagonal system, lattice spacing d is given by the following mathematical equation **[9]**:

$$\frac{1}{d^2}=\frac{4}{3}\left(\frac{h^2+hk+k^2}{a^2}\right)+\frac{l^2}{c^2}..............(1)$$

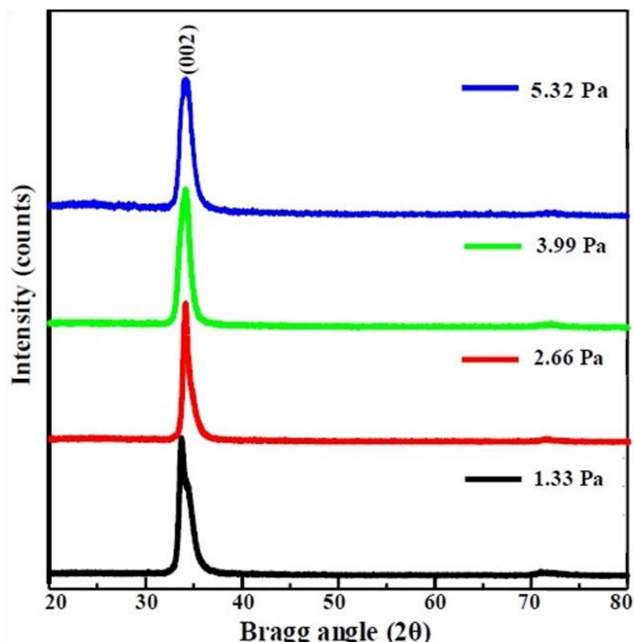

Fig. 1. The XRD patterns of the Al:ZnO thin films indicating (002) plane growth.

Where h, k, l are the Miller indices of the plane. The lattice constant, c is calculated using the values of d in equation 1. The Crystallite size (l) of the grown films is estimated by using Debye-Scherrer formula relation **[10]**:

$$l=\left(\frac{0.9\lambda}{\beta cos\theta}\right).......................(2)$$

Where λ is the wavelength of X-rays used = 0.154 nm, θ is the Bragg diffraction angle and β is the width at the half maxima of the XRD peak (002). Crystallite size means the dimension of the coherent diffracting domain. The calculated values of interplanar distance (d), lattice constant (c) and crystallite size of the grown films are listed in **Table 2**.

The smaller is the FWHM better would be the crystallinity. The increase in lattice constant c, as compare with ZnO (0.5209 nm), is due to incorporation of Al^{3+} ions at interstitial position. The dislocation density (δ), defined as the length of dislocation lines per unit volume, is estimated using the equation **[11]**:

$$\delta=\frac{1}{l^2}..........................(3)$$

The strain (ε) of the thin films can be computed using the following relation:

$$\varepsilon=\frac{\beta\cos\theta}{4}...............(4)$$

The obtained values of dislocation density (δ) and the strain (ε) are listed in **Table 2**.

Table 2. Interplanar distance, lattice constant, crystallite size, dislocation density and strain calculated from XRD data analysis.

Sample	Interplanar distance, d (nm)	Lattice constant, c (nm)	FWHM (β)	Crystallite size (nm)	Dislocation density, δ (nm^{-2})	Strain, ε
1.33 Pa	0.2619	0.5238	0.5722°	14.362	48.48×10^{-4}	24.13×10^{-4}
2.66 Pa	0.2614	0.5228	0.5914°	13.899	51.76×10^{-4}	24.93×10^{-4}
3.99 Pa	0.261	0.522	0.6217°	13.223	57.19×10^{-4}	26.21×10^{-4}
5.32 Pa	0.2607	0.5214	0.6843°	12.015	69.27×10^{-4}	28.84×10^{-4}

Fig. 2 shows the 3-dimensional grain formation of the thin films obtained from AFM analysis. The AFM images depict the uniform grain distribution and the smooth surface. The thin films exhibit dense and continuous morphologies with crystalline nano-structures. The z-dimension shows the particle heights. AFM analysis verifies that the products have well-defined shape, uniform size and good dispersion. The grown microstructures of the films are distinctly affected by the process controlling the deposition rate.

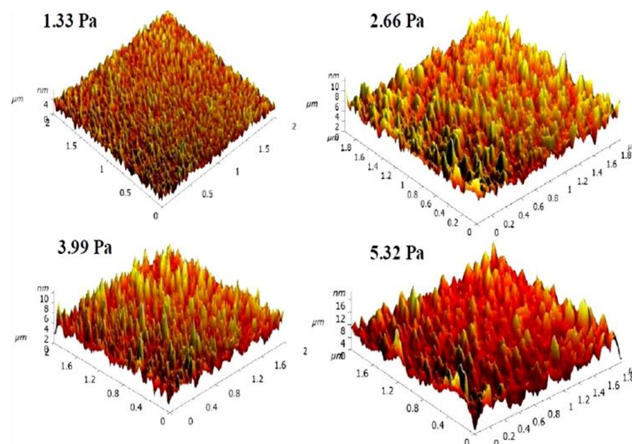

Fig. 2. 3-D AFM images of the deposited thin films describing the grain distribution and the particle height from the z-dimension.

The calculated parameters, grain size and roughness values obtained from AFM analysis is listed in **Table 3**.

 Copyright © 2015 VBRI Press

The nucleation and growth process of the thin films involve nuclei formation, growth and coalescence **[12]**. For the as grown thin film grains are not completely formed, thus annealing is required for the crystallinity and the homogeneous grain growth. The as-grown films are having a good adhesion to the glass substrates. The surface roughness histograms of the deposited thin films are described by **Fig. 3**. Low surface roughness enhances the optical properties by lowering the surface scattering.

Table 3. The geometrical parameters calculated from AFM analysis of the deposited thin films.

Sample	Mean height of Grain, h (nm)	Mean diameter of grain, D (nm)	Aspect ratio D/h	Average Grain size (nm)	Particle density = No. of grains/ Area (μm^{-2})	Surface Coverage = (Area of 1grain × No. of grains × 100)/ Total area	Roughness (nm)	
							Average	Rms
1.33 Pa	3.84	41	10.68	3.43	169.5	63.80%	0.641	0.804
2.66 Pa	5.67	55	9.7	5.35	73.5	56.75%	0.898	1.132
3.99 Pa	5.75	31	5.39	5.31	115	53%	0.985	1.252
5.32 Pa	10.07	32	3.18	9.44	86.75	47.35%	1.698	2.198

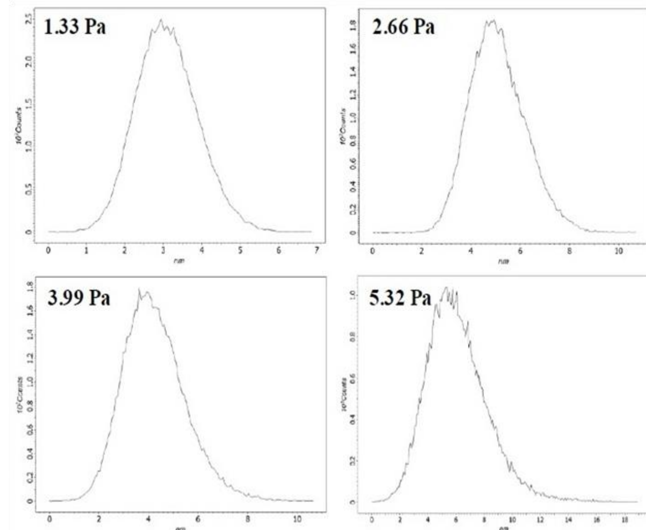

Fig. 3. The roughness histogram of the thin films obtained from AFM analysis.

Optical measurements and band gap

The optical transmittance versus wavelength spectra of the deposited thin films is described by **Fig. 4**. From the transmission spectra it is clearly observed that all the thin films exhibit good transparency over 60-80% in the visible region and a sharp UV absorption cut-off at wavelength <400 nm. High optical transparency and electrical conductivity of Al:ZnO thin films are applicable for transparent conducting oxide (TCO) layer of heterojunction solar cells. Al:ZnO thin films may be considered as a better replacement over TCO Indium tin oxide (ITO) films.

The transmittance curves show a well defined interference fringe pattern, indicating the good optical quality of the films. For the thin films deposited on glass substrates, transmittance minimum (T_{min}) in the fringe pattern, is related to the refractive index (n) by the following mathematical relation **[13]**:

$$T_{\min} = \frac{6n^2}{n^4 + 3.35n^2 + 2.25} \quad \text{.................(5)}$$

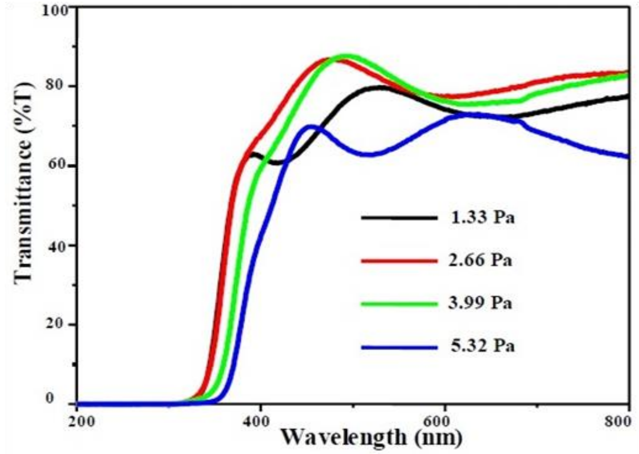

Fig. 4. Optical transmittance versus wavelength curves showing a well defined fringe pattern.

Refractive index (n) is related to fringe order (h) and film thickness (t) as:

$$2nt = h\lambda_{\min} \quad \text{.....................(6)}$$

$$2nt = \left(h + \frac{1}{2}\right)\lambda_{\max} \quad \text{..........(7)}$$

From equation 5, 6 and 7 we have calculated values of film thickness (t) and refractive index (n). O_2 is used as a reactive gas for deposition. The reaction rate increases with PO_2. It enhances the probability of oxygen atoms to react with the Zn^{+2} ions, implies more thick films at high pressure. The calculated values of film thickness, t and refractive index, n are listed in **Table 4**.

The optical absorbance and reflection versus wavelength spectra are shown in **Fig. 5** (**a** and **b**). The thin films show strong absorption at wavelength 398, 403, 414, 428 nm respectively for 1.33, 2.66, 3.99 and 5.32 Pa samples respectively. Deposited Al:ZnO thin films show low optical reflection, values < 20%, that is good for device applications. The absorption coefficient α is calculated using Lambert's formula **[14]**:

$$\alpha = \frac{1}{t}\ln\left(\frac{1}{T}\right) \qquad \text{................(8)}$$

where, t is the thickness of thin film and T is the transmittance values.

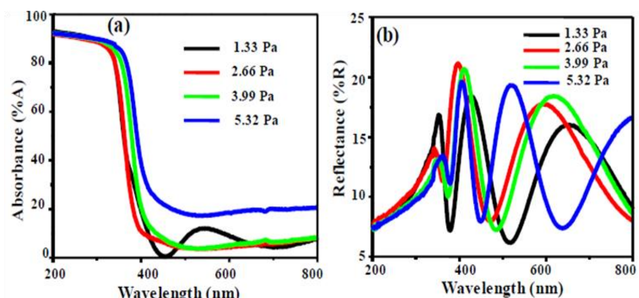

Fig. 5. (a) Optical Absorbance and (b) reflectance versus wavelength spectra of the as-grown Al:ZnO thin films.

 Copyright © 2015 VBRI Press

The optical band gap is calculated from Tauc's model and the Davis and Mott model given by the equation **[8, 14]**:

$$\alpha h\nu = D(h\nu - E_g)^n \text{ .... (9)}$$

Where hυ is the photon energy, E_g is the optical band gap, and D is the constant, n=1/2 for direct band gap semiconductors. Band gap can be calculated from the Tauc's plot $(\alpha h\upsilon)^2$ versus hυ, and by extrapolating the linear portion of the absorption edge to find the intercept with energy axis, **Fig. 6**. These thin films have a lower band gap as compared with the ZnO (3.37 eV) thin films, due to band edge bending by Al-doping **[2]**. In Al:ZnO, Al^{3+} ion replaces one Zn^{2+} and one excess electron is produced. These excess electrons form a band below the conduction band which results in band edge bending. The further decrease in the band gap with an increase in oxygen gas pressure is due to the contributing electrons from oxygen ions. Formation of localized energy states below the conduction band, leads to the formation of a band tail, thereby resulting in the band gap lowering. The calculated values of the band gap of the thin films are 3.16, 3.12, 3.01, 3.0 eV for 1.33 to 5.32 Pa oxygen gas pressure respectively. The lowering in band gap also results from reduction of crystallite size due to quantum size effects (QSE) **[9]**. The density of states is modified by the particle size of the nano grains, which engineered the band gap. Decrease in band gap is also attributed to electron-electron and electron-impurity scattering **[8]**. UV absorption enables Al:ZnO thin for energy conversion applications.

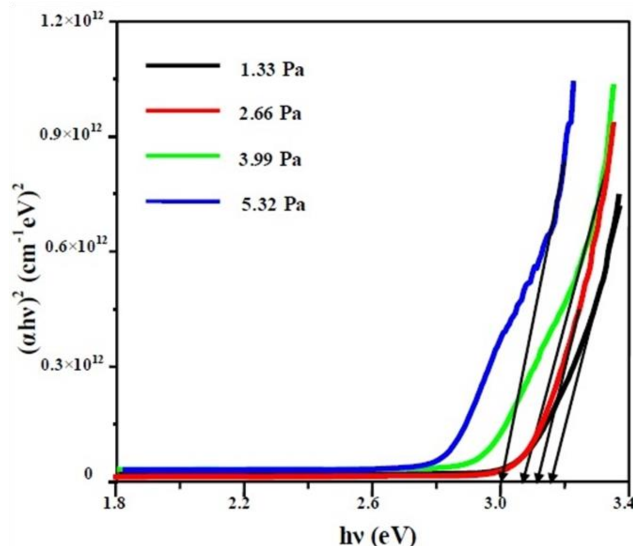

Fig. 6. Optical band gap obtained using Tauc's plot.

Photoluminescence (PL) measurements

Photoluminescence (PL) is a good study to characterize optical quality of semiconductors. **Fig. 7** depicts the room temperature PL spectra of the deposited thin films at excitation wavelength λ_{ex} = 320 nm. All the thin films show a sharp emission peak at wavelength ~ 390 nm (3.17 eV), the UV emission. This emission peak corresponds to the band gap of the Al:ZnO and is the characteristic emission peak. The UV emission peak is therefore considered to originate from the band-edge exciton emission. There are visible emission peaks which are originating due to transitions from shallow energy levels. These shallow energy levels correspond to various defect states such as Oxygen (O), Zinc (Zn) vacancies and interstitials or surface states. ZnO is a n-type semiconductor, therefore Zinc interstitials (Zn_i) and oxygen vacancies act as main donor impurities whereas Zn vacancies and oxygen interstitial act as main acceptor impurities **[9]**. Zinc interstitial (Zn_i) produces a shallow donor level at 0.5 eV below the bottom of the conduction band. Shallow acceptor levels are created at 0.3 eV and 0.4 eV above the top of the valence band (VB) due to zinc vacancy (V_{Zn}) and oxygen interstitial (O_i), respectively **[15]**. Photons emitting due to transitions from these shallow energy levels give visible emission peaks at wavelength 470 and 495 nm respectively. These visible emission peaks correspond to blue light. Blue emission peaks are assigned to electron transition from Zn_i level to top of the valence band. There are small peaks detected at wavelength 510 and 520 nm, correspond to green emission. Green emission peak results from the recombination of a photo generated hole with a singly ionized oxygen vacancy **[16]**. The very low intensity of this emission peak is the clear indication of low concentration of oxygen vacancies in the films. These emission peaks in the visible region enables Al: ZnO thin films for application as a light emitting diodes (LED) and laser diodes (LD). PL emission peaks are strongly dependent on the crystalline nature of the films. Various optoelectronic and photovoltaic devices rely on PL emission peaks of Al:ZnO thin films **[17]**.

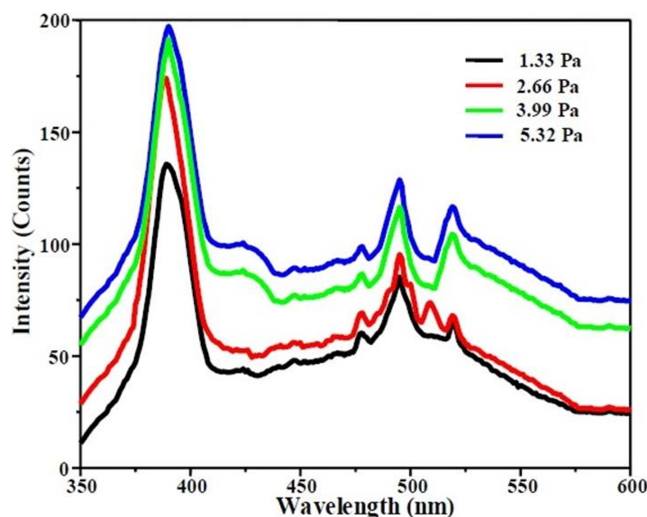

Fig. 7. Photoluminescence spectra of thin films at λ_{ex} = 320 nm.

Electrical properties

The room temperature I-V plots of the thin films are described in **Fig. 8**. The thin films exhibit ohmic conduction behavior. The electron donor states are provided by the native defects such as zinc interstitials (Zn_i). The decrease in resistivity with the increase in gas pressure is observed, which is attributed to a reduction in oxygen vacancies that can act as centers for electron traps. The abrupt terminations on the surface of the semiconductor cause distruption of potential function would create discrete energy states within the band gap

Copyright © 2015 VBRI Press

which were called surface states and could trap the free carriers **[18]**. Reduced resistivity of the Al-doped ZnO films is attributed to the increased free carrier concentrations, which originated from desorption of the negatively charged oxygen species from the grain boundary surfaces **[19]**. The preferred c-axis orientation of the thin films suggests that the crystal orientation plays an important role in the conductivity **[20]**. The probability of scattering of carriers is low for highly oriented thin films. The calculated value for resistivity of these thin films is given by this relation **[21]**:

$$\rho = \frac{\pi t}{\ln 2} \times \left(\frac{V}{I} \right) \qquad (10)$$

where, V is the voltage measured across the inner probes, I is the current applied between the outer probes, and t is the thickness of the thin film. The calculated values of resistivity are listed in **Table 4**. The obtained sheet resistance of the thin films is <100 Ω/sq. This low resistivity Al:ZnO thin films found applicability in ZnO based unipolar devices such as a Schottky barrier diode, thin film transistor, and metal–insulator-semiconductor (MIS) diodes **[22-25]**.

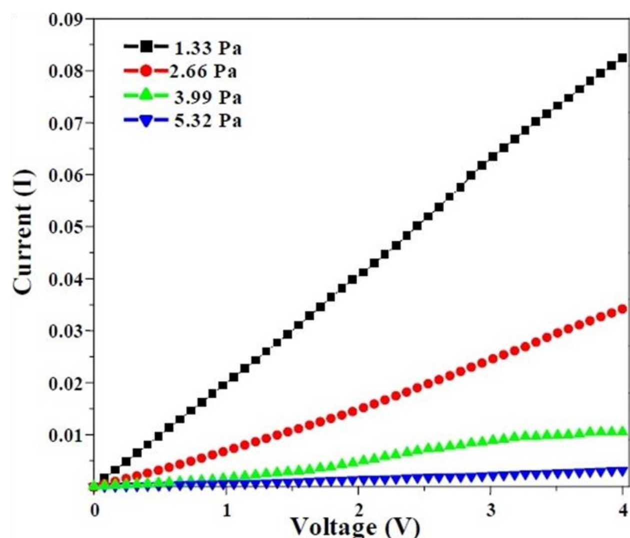

Fig. 8. The electrical properties (I-V plots) examined by Four Probe method.

Table 4. Thickness (t), Refractive index (n) and Band gap calculated from Optical data and Resistivity (ρ) calculated from room temperature I-V characteristics.

Sample	T_{min}	Refractive Index, n	Thickness, t (nm)	Band Gap, E_g (eV)	Resistivity, ρ (Ω-cm)
1.33 Pa	0.7234	2.133	300.72	3.06	14.37×10^{-2}
2.66 Pa	0.7735	1.984	303.97	3	3.88×10^{-2}
3.99 Pa	0.7541	2.041	308.33	2.94	1.57×10^{-2}
5.32 Pa	0.6269	2.438	313.98	2.9	0.65×10^{-2}

Conclusion

Al:ZnO thin films are successfully deposited on glass substrates using PLD. XRD analysis confirms that the films are oriented along (002) plane with hexagonal wurtzite crystal structure. The AFM results indicate homogeneous grain growth along c-axis, parallel to the substrate. The observed crystallographic property and surface morphology of deposited Al:ZnO thin films are found to be affected considerably by PO_2. The surface morphology and crystallinity of the Al:ZnO thin films are very important for their optical applications. The thin films exhibit significant optical properties with high optical transmittance in the visible region and a sharp UV absorption. Band edge bending is observed due to Al-doping in ZnO. Room temperature photoluminescence indicates strong UV and visible emission peaks. Visible emission peaks correspond to defect related emissions, which make these thin films important for optoelectronic applications. The I-V properties confirms the electronic device applications of the Al:ZnO thin films. Doping-effects have resulted in an enhanced electrical conductivity of Al:ZnO thin films. The deposited thin films exhibit the essential properties of a TCO with good transmittance in the visible and near infrared (NIR) region, low resistivity, and textured surface with excellent light-scattering.

Acknowledgements

The author Gurpreet Kaur gratefully acknowledges to the Department of Science and Technology for their financial support of INSPIRE fellowship for this work. The author wishes to thanks Dr. Anirban Mitra for the guidance provided in this research work.

Reference

1. Sivalingam, K.; Shankar, P; Mani, G.K.; John Bosco BalaguruRayappan, J.B.R; *Mater. Lett.* **2014,** *134*, 47. **DOI:** 10.1016/j.matlet.2014.07.019
2. Gondoni, P.; Ghidelli, M.; Fonzo, F.D.; Russo, V.; Bruno, P.; Marti-Rujas, J.; C.E. Bottani; Bassi, A.L.; Casari, C.S.; *Thin SolidFilm,* **2012,** *520,* 4707. **DOI:** 10.1016/j.tsf.2011.10.072
3. Ahmad, M.; Ahmed, E.; Zhang, Y.; Khalid, N.R.; Xu, J.;Ullah, M.; Hong, Z.; *Curr. Appl. Phys.,* **2013,** *13*, 697. **DOI:** 10.1016/j.cap.2012.11.008
4. 4.Lu, Y.M.; Li, X.P.; Su, S.C.; Cao, P.J.; Jia, F.; Han, S.; Zeng,Y.X.; Liu, W.J.; Zhu, D.L. ; *J. Lumin.,* **2014**, *152*, 254. **DOI:** 10.1016/j.jlumin.2013.10.023
5. Mereu, R.A.; Mesaros, A.; Vasilescu, M.; Popa, M.; Gabor,M.S.; Ciontea, L.; Petrisor, T.; *Ceram. Int.,* **2013**, *39*, 5535. **DOI:** 10.1016/j.ceramint.2012.12.067
6. Mahroug, A.; Boudjadar, S.; Hamrit, S.; Guerbous, L.; *Mater.Lett.,* **2014**, *134*, 248. **DOI:** 10.1016/j.matlet.2014.07.099
7. Manikandan, E.; Murugan, V.; Kavitha, G.; Babu, P.;Maaza, M.; *Mater. Lett.*, **2014**, *131*, 225. **DOI:** 10.1016/j.matlet.2014.06.008
8. Guillen, C.; Herrero, J.; *Vacuum,* **2010**, *84*, 924. **DOI:** 10.1016/j.vacuum.2009.12.015
9. Zhang, X.; Ma, S.; Yang, F.; Zhao, Q.; Li, F.; Jing Liu;*Ceram. Int.,* **2013**, *39*, 7993. **DOI:** 10.1016/j.ceramint.2013.03.066
10. Benramache, S.; Temam, H.B.; Arif, A.; Guettaf, A.;Belahssen, O.; *Optik,* 2014, *125*, 1816. **DOI:** 10.1016/j.ijleo.2013.09.024
11. Kayani, Z.N.; Afzal, T.; Riaz, S.; Naseem, S.; *J. Alloys Compd.* **2014**, *606*, 177. **DOI:** 10.1016/j.jallcom.2014.04.039
12. Kumar, V.; Kumar, V.; Som, S.; Yousif, A.; Singh,N.; Ntwaeaborwa, O.M.; Kapoor, A.; Swart, H.C.; J.ColloidInterf. Sci., 2014, *428*, 8. **DOI:** 10.1016/j.jcis.2014.04.035
13. Martil, I.; Gonzalez Diaz, G,G,; *Am. J. Phys.,* **1992**, *60*, 83. **DOI:** 10.1119/1.17049
14. Wang, T.; Liu, Y.; Fang, Q.; Wu, M.; Sun, X.; Fei Lu; *Appl.Surf. Sci.* **2011**, *257*, 2341.

 Copyright © 2015 VBRI Press

DOI: 10.1016/j.apsusc.2010.09.100

15. Karaka, N.; Samanta, P.K.; Kundu, T.K.; *Optik,* **2013**, *124*, 6227.
DOI: 10.1016/j.ijleo.2013.05.019
16. Kim, H.W.; Kebede, M.A.; Kim, H.S.; *Curr. Appl. Phys.,* **2013**, *10*, 60.
DOI: 101016/j.cap.2009.04.012
17. Singh, S.; Chakrabarti, P.; *Superlattice Microst.,* **2013**, *64*, 283.
DOI: 10.1016/j.spmi.2013.09.031
18. Dong, B.Z.; Fang, G.J.; Wang, J.F.; Guan, W.J.; Zhao, X.Z.; *J. Appl. Phys.,* **2007**, *101*, 033713.
DOI: 10.1063/1.2437572
19. Zhong, W.W.; Liu, F.M.; Cai, L.G.; Ding, P.; Zhou, C.C.; Zeng, L.G.; Xue-Quan Liu; Yi Li; *J.Alloys Compd.,* **2011**, *509*, 3847.
DOI: 10.1016/j.jallcom.2010.12.118
20. Oh, B.Y.; Jeong, M.C.; Kim, D.S. ; Lee, W. ; Myoung, J.M.; *J. Cryst. Growth, 2005, 281, 475.*
DOI: 10.1016/j.jcrysgro.2005.04.045
21. Dieter K. Schroder *Semiconductor Material and Device Characterization Third Edition* (Canada: *A John Wiley & Sons; Inc.; Publication)* G. Telecki, **2006**, pp. 10.
ISBN: 978-0-471-73906-7
22. Ozgur, U.; Alivov, Ya.I. ; Liu, C.; Teke, A. ; Reshchikov, M.A.; Dogan, S.; Avrutin, V. ; Cho, S.J.; Morkoc, H. ; *J. Appl. Phys.,* **2005**, *98*, 041301.
DOI: 10.1063/1.1992666
23. B. Angadi, B.; Park, H.C.; Choi, H.W. ; Choi, J.W.; Choi, W.K.; *J. Phys. D: Appl. Phys.,* **2007**, *40*, 1422.
DOI: 10.1088/0022-3727/40/5/016
24. Zhang, J.; Yang, H.; Zhang, Q.; Dong, S.; Luo, J.K.; *Appl. Surf. Sci.,* **2013**, *282*, 390.
DOI: 10.1016/j.apsusc.2013.05.141
25. Young, S.J.; Ji, L.W.; Chang, S.J.; Liang, S.H.; Lam, K.T.; Fang, T.H.; Chen, K.J.; Du, X.L.; Xue, Q.K.; *Sens. Actuators A,* **2008**, *141*, 225.
DOI: 10.1016/j.sna.2007.06.003

Advanced Materials Letters

Publish your article in this journal

ADVANCED MATERIALS Letters is an international journal published quarterly. The journal is intended to provide top-quality peer-reviewed research papers in the fascinating field of materials science particularly in the area of structure, synthesis and processing, characterization, advanced-state properties, and applications of materials. All articles are indexed on various databases including DOAJ and are available for download for free. The manuscript management system is completely electronic and has fast and fair peer-review process. The journal includes review articles, research articles, notes, letter to editor and short communications.

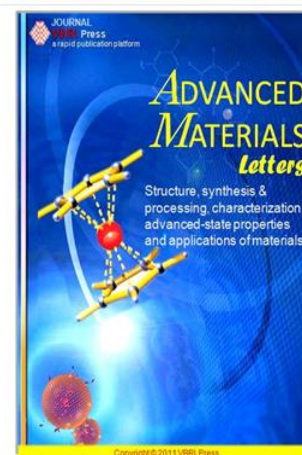

Copyright © 2015 VBRI Press